

Structural, Emission & Dielectric Properties of $\text{Sm}^{3+}:\text{SrTiO}_3$ Ceramic Powders

J. Guravamma¹, B. H. Rudramadevi²

Assistant Professor, Department of Physics, Sri Venkateswara University, Tirupati, India¹

Research Scholar, Department of Physics, Sri Venkateswara University, Tirupati, India²

Abstract: SrTiO_3 and $\text{Sm}^{3+}:\text{SrTiO}_3$ ceramic powders were prepared by using a conventional solid state reaction method. The Structural, photoluminescence and dielectric properties have been studied for those ceramic powders. The XRD study reveals that the formation of mono phasic compounds and indicated structure to be changed from cubic to tetragonal by adding the samarium dopant. The Raman studies explain the structural phase transition and SEM with EDS explains the morphological and elemental analysis. From the SEM analysis reveals that the samarium doped strontium titanate grain size is increased compared to the pure strontium titanate. Under an excitation of 410 nm, corresponding to this transition is (${}^6\text{H}_{5/2} \rightarrow {}^4\text{L}_{13/2}$) the emission wavelengths will be occurred. Among the all emission wavelengths, the 602 nm (${}^4\text{G}_{5/2} \rightarrow {}^6\text{H}_{7/2}$) is a bright reddish orange emission wavelength. We also investigated the dielectric properties as a function of frequency in the range of (100Hz – 1MHz) at room temperature. For dielectric properties, the dielectric constant (ϵ_r), tangent loss ($\tan \delta$) and as well as AC conductivity were measured. These dielectric properties can be used in energy storage applications.

Keywords: Rare earth ion, Photoluminescence, Dielectric properties, SrTiO_3 .

I. INTRODUCTION

The cubic perovskite SrTiO_3 is one of the most ceramic materials for dielectrics due to their energy storage applications for high voltage capacitors [1]. During the past several decades divalent alkaline earth metals Ba^{2+} , Ca^{2+} substituting for A-site Sr^{2+} ion and as well as tetravalent ions Zr^{4+} ion substituting the Ti^{4+} ion were studied the results was found to be enhanced the energy storage property of the high voltage capacitors [2-4]. On the other hand trivalent rare earth ions doped strontium titanate much attention due to there in recent years. Shi at al. Reported that Er^{3+} ion gradually transformed to the Sr/Ti in STO and the light response rays effectively responded from ultraviolet to the visible light for photocatalystics [5]. Based on the above considerations our work has been concentrated on trivalent rare earth ion samarium doped strontium titanate ceramics. The particular importance of that samarium is doped with strontium vacancies because of it compensating the charge unbalance induced by trivalent Sm^{3+} substituting for divalent Sr^{2+} . The perovskite phase $\text{Sr}_{1-x}\text{M}_x\text{TiO}_3$ ($\text{M}=\text{Sm}^{3+}$) ceramics have been reported for their excellent photoluminescence and dielectric properties [6]. Among them tetragonal distorted perovskite $\text{Sr}_{0.8}\text{Sm}_{0.2}\text{TiO}_3$ is widely used for potential candidate material for dielectric energy storage capacitor applications, because it was high dielectric constant.

II. EXPERIMENTAL DETAILS

Materials: Sm_2O_3 (99.9% purity), SrCO_3 and TiO_2 (Annular grade) were used as the raw chemicals to prepare the SrTiO_3 and (0.2 mol %) $\text{Sm}^{3+}:\text{SrTiO}_3$ ceramic powders by a solid state reaction method.

Preparation: Suitably weighed chemicals were mixed with acetone for homogeneous mixing in an agate mortar for 1hr and later it was collected into a porcelain crucible for its appropriate heating. The temperature was gradually raised from room temperature to 1150°C, at this temperature the chemical mixture was kept for about 4h in an ambient atmosphere with intermediate grinding. After that, the resultant powders were ground and pelletized at 50 MPa pressure into disks of 10 mm in diameter and 3 mm in thickness. Again the pellets was sintered at furnace 900°C for 2 hours. The final products obtained were used for further characterizations.

III. CHARACTERIZATION TECHNIQUES

The structure of the ceramic powder is examined by powder X-ray diffraction technique using X-ray diffractometer with nickel filtered Cu K_α radiation (Model Philips Expert Pro). The Raman spectrum on a job in Yvonne Horiba (LABRAM HR-800) Micro Raman spectrometer attached with a He-Ne laser (632.8 nm) as the excitation source. SEM and EDAX studies were carried out using Philips XL30 ESEM and JEOL JSM 840 electron microscope. Both the excitation and emission spectra of these ceramic powders were recorded on a SPEX Fluorolog-2 Fluorimeter (Model-

II) with a Xe-arc lamp (150W) in the wavelength region of 320 - 580 nm for excitation and 540 - 740 nm for emission spectra respectively. Emission decay curves were obtained with a phosphorimeter attachment to the system fitted with a Xe-flash lamp (50W) in the place of CW source. The dielectric constant (ϵ'), dielectric loss factor ($\tan \delta$) and Ac conductivity of the sintered pellets were measured using an impedance analyzer (Model PSM 1700 RS 232).

IV. RESULTS AND DISCUSSIONS

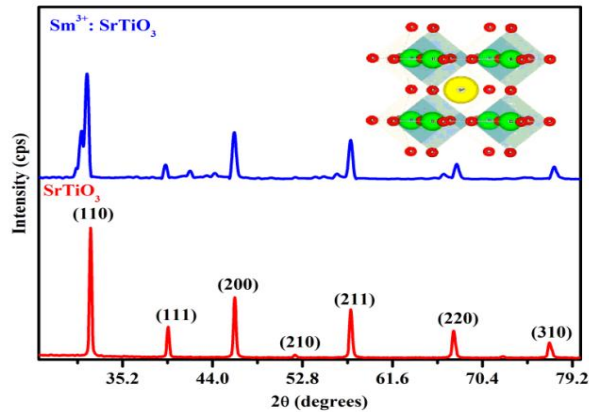


Fig.1 XRD profile of SrTiO_3 & $\text{Sm}^{3+}:\text{SrTiO}_3$ ceramic powders (inset figure shows perovskite SrTiO_3)

The fig.1 shows the prepared samples were analyzed by powder X-ray diffraction using $\text{Cu-K}\alpha$ radiation ($\lambda=1.5406 \text{ \AA}$) with 2θ ranging from 20° to 80° with a scan rate of 0.02 steps per second. Figure 1 shows the XRD pattern of the SrTiO_3 and $\text{Sm}^{3+}:\text{SrTiO}_3$ ceramic powders and they are indexed on the basis of the reflections from the JCPDS file no. 84-0443. The major phase was identified to be cubic SrTiO_3 with, (110), (111), (200), (210), (211), (220) and (310) reflections appearing in 32.0° , 39.7° , 46.1° , 52.0° , 57.5° , 67.6° , and 77.1° 2θ positions respectively. For samarium doped strontium titanate phase transition will be occurred. The phase transition is important role in the Powder diffraction this is mainly classified into two types. The first transition is reconstructive nature in the crystal structure and second transition is displace nature. The powder diffraction is very useful in first order transition. The main difference between the crystal structure and phases means it is difficult to use the structural information obtained from the one phases to second one. The unit cell of the both the phases often related to the space group symmetries. The symmetries changes from the one crystal system to another one that is cubic to tetragonal or orthorhombic or monoclinic. For cubic \rightarrow tetragonal system is presented in the $\text{Sm}^{3+}:\text{SrTiO}_3$ powder diffraction. In this system the (100) cubic peak splits into two peaks with indices 100 and 001 in that case $a \neq c$. Likewise the 110 cubic peak will split into two peaks with indices 110 and 101. However, the 111 cubic peak will not split under this symmetry transformation. The 200 cubic peak will be split into two peaks with indices 200 and 002. The inter planar spacing for (011); i.e., d_{110} was calculated from the corresponding 2θ position using Bragg law as described in the experimental methodology section and found to be 2.7939 \AA and then the SrTiO_3 lattice constant, the crystallite size will be calculated is about 3.898 \AA and 54 nm . The figure 1 inset figure shows the simulated perovskite lattice of the SrTiO_3 ceramic powder shows the illustration of the SrTiO_3 unit cell. The unit cell was modeled through a program called Visualization for Electronic and Structural Analysis (VESTA). From the figure it is clear that the A site cation Sr is surrounded by O atoms and B site ion T is surrounded six O atoms. The atomic arrangement of strontium titanate structure is quite similar to that of Perovskite structure. The perovskite strontium titanate is cubic in nature due to the $\text{Pm}\bar{3}\text{m}$ space group. The lattice parameters of SrTiO_3 are $a=b=c=3.898 \text{ \AA}$.

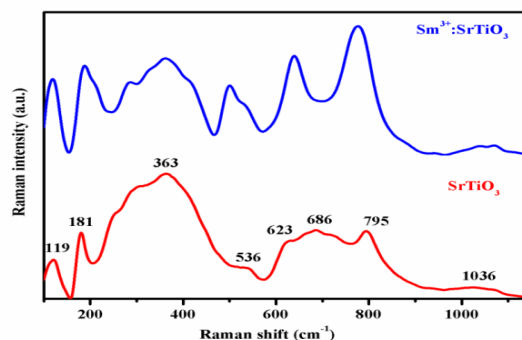


Fig.2 Raman spectrum of SrTiO_3 & $\text{Sm}^{3+}:\text{SrTiO}_3$ ceramic powders

The fig.2 shows the Raman spectrum for SrTiO₃ and Sm³⁺: SrTiO₃ ceramics. Raman spectroscopy is used to investigate the phonon properties and structural phase transition. The phonon anomalies and structural distortion due to existence of polar micro regions. The spectra exhibit the broad continuum in the range of 100-1150 cm⁻¹. The 100-600 cm⁻¹ region is called the first order Raman modes and region 600-1150 cm⁻¹ region is called the second order Raman modes. The first order Raman modes, five bands are occurring denoted by 119, 181, 363 and 536 cm⁻¹. Among them the bands at 119, 181, 363, and 536cm⁻¹ are ascribed to TO₁, TO₂, TO₃ and TO₄ modes respectively. While the bands at 623 and 795 cm⁻¹ are the LO₂ and LO₄ modes respectively. The first order Raman modes show a significant increasing the Raman intensity compared to that of by adding the do part of the SrTiO₃. Due to because of strain effect of the oxygen vacancies of the strontium titanate [7]. And the second order Raman modes of the intensity were decreased compared to that of Sm³⁺: SrTiO₃ because the intensity of the Raman scattering gets weaker. The broad Raman shift completely disappeared at 1150 cm⁻¹. Which might be related to the transition from polar micro regions to polar macro regions in the perovskite strontium titanate.

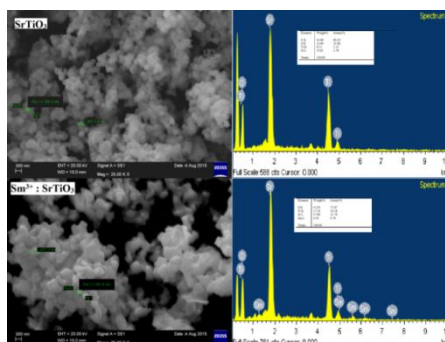


Fig.3 SEM & EDS images of the SrTiO₃ & Sm³⁺:SrTiO₃ ceramic powders

The fig. 3 shows the SEM & EDS images of the pure SrTiO₃ and Sm³⁺: SrTiO₃ Ceramic powders. The SEM images of the samples had obvious pores or displayed homogeneous microstructure. The grain size of SrTiO₃ and Sm³⁺: SrTiO₃ samples are about 184.3 and 241.4 nm respectively. The grain size of the samarium doped strontium titanate is increases compared to the pure strontium titanate. We believe that these fine particles belong to the second phase and that their sizes are on the nanometer scale. These nano size particles increase the scattering centers as well as decrease the thermal conductivity and electrical conductivity. The energy dispersive x-ray spectroscopy (EDS) spectrum shows the elements that are present in the specimens prepared.

The fig. 4 shows the emission spectra of Sm³⁺: SrTiO₃. Excited at 410 nm, it is drawn to the 0.2 single concentrations it is the most intense one. These four obvious sharp emission peaks are located at 567, 602, 649 and 707 nm corresponds to the transitions are $^4G_{5/2} \rightarrow ^6H_{5/2}$, $^4G_{5/2} \rightarrow ^6H_{7/2}$, $^4G_{5/2} \rightarrow ^6H_{9/2}$ and $^4G_{5/2} \rightarrow ^6H_{11/2}$ intra-4f transitions of Sm³⁺: SrTiO₃ respectively. Among these emission bands, the reddish orange color wavelength is 602 nm corresponding transitions are $^4G_{5/2} \rightarrow ^6H_{7/2}$. Follow the selection rule of $\Delta J = \pm 1$ indicating it as a magnetic dipole (MD) and allowed transitions but it is an electric dipole (ED) dominated, therefore, it can be stated that but it is a partly magnetic dipole and it is partly Electric dipole one. The other transition $^4G_{5/2} \rightarrow ^6H_{9/2}$ is purely an Electric dipole one which is sensitive to the crystal field [8]. Generally, the intensity ratio of the Electric dipole (ED) and magnetic dipole (MD) transitions could be used to understand the symmetry of the local environment of the trivalent 4f ions in the host matrix investigated. The intensity of the Electric dipole transition is greater than that of Magnetic dipole transition; it can occupy the more asymmetry nature [9].

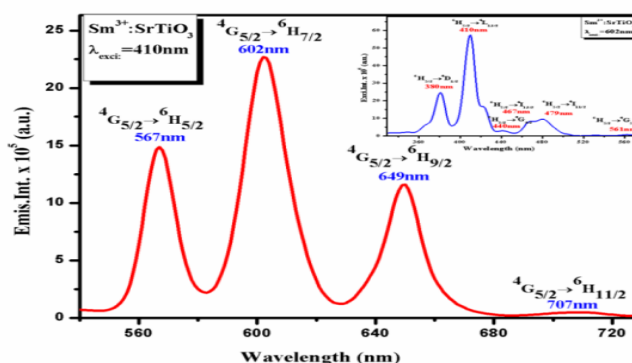


Fig. 4 Emission spectrum ($\lambda_{exc} = 410\text{nm}$) of Sm³⁺:SrTiO₃ ceramic powder (inset figure: Excitation spectrum ($\lambda_{emi} = 602\text{nm}$))

The inset figure shows the excitation spectrum of $\text{Sm}^{3+}:\text{SrTiO}_3$ these spectra consist to the ground state $^6\text{H}_{5/2}$ to the various excited states. The excitation spectra consists of the several peaks these are 380, 410, 440, 467, 479, and 561 nm corresponds to the transitions are $^6\text{H}_{5/2} \rightarrow ^4\text{D}_{5/2}$, $^6\text{H}_{5/2} \rightarrow ^4\text{L}_{13/2}$, $^6\text{H}_{5/2} \rightarrow ^4\text{G}_{9/2}$, $^6\text{H}_{5/2} \rightarrow ^4\text{I}_{13/2}$, $^6\text{H}_{5/2} \rightarrow ^4\text{I}_{11/2}$, and $^6\text{H}_{5/2} \rightarrow ^4\text{G}_{5/2}$. The strongest excitation peak is noticed that the 410 nm corresponding this transition is $^6\text{H}_{5/2} \rightarrow ^4\text{L}_{13/2}$.

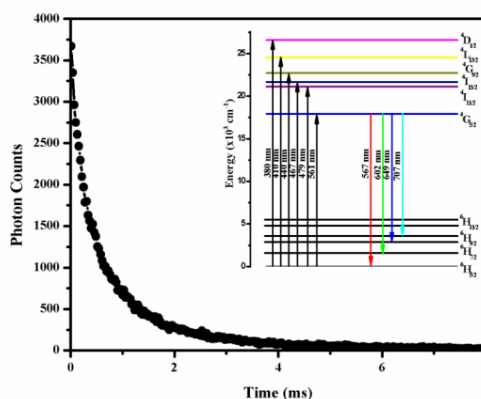


Fig.5 Decay curve of $\text{Sm}^{3+}:\text{SrTiO}_3$ ceramic powder (inset figure shows an energy level diagram of the $\text{Sm}^{3+}:\text{SrTiO}_3$ ceramic powder)

The fig.5 shows the decay curve of the $\text{Sm}^{3+}:\text{SrTiO}_3$ ceramic powder. Where also investigated under the excitation of 410 nm. The decay curve is well fitted to a single exponential decay. Is obtained by fitting the decay curve to the equation as $I_t = I_0 \exp(-t/\tau)$ where t is time I_t and I_0 is intensity at time t and 0. τ is defined as the luminescence lifetime respectively. These are plotted for the prominent emission transition $^4\text{G}_{5/2} \rightarrow ^6\text{H}_{7/2}$ at 602 nm. The inserted lifetime was found to be 0.595 ms. The inset figure shows the energy level diagram of the $\text{Sm}^{3+}:\text{SrTiO}_3$ ceramic powder. The energy level scheme explains the excitation and emission wavelength mechanism of the investigated materials.

The fig.6 shows the luminescence color of samples (excitation wavelength, 410 nm) has been characterized by the CIE 1931 chromaticity diagram. The color coordinates x and y calculated are found to be 0.47 and 0.36 as indicated in fig 6. Generally, monochromatic sources ($\Delta\lambda \rightarrow 0$) are located on the perimeter of the chromaticity diagram. The color location moves towards the center of the chromaticity diagram, when spectral and width of a source gets broader.

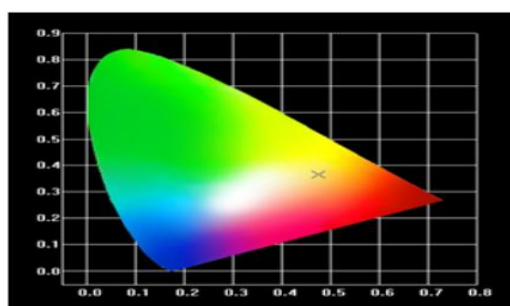


Fig.6 Chromaticity diagram of $\text{Sm}^{3+}:\text{SrTiO}_3$ ceramic powder

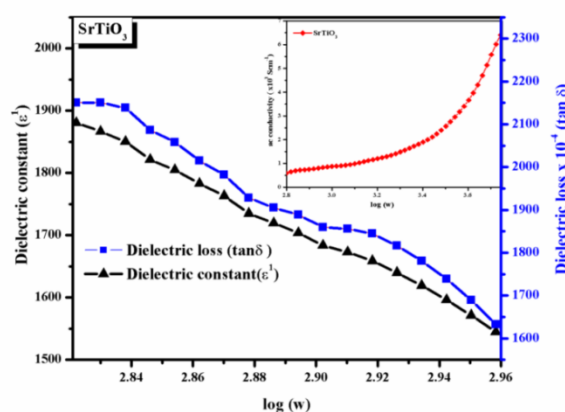


Fig.7 Dielectric constant (ϵ'), loss factor ($\tan\delta$) & ac conductivity (inset figure) of SrTiO_3 ceramic powder

Hence, for white light emission, the coordinates are located near the center of the chromaticity diagram. In the present work, for all the ceramic powders, the color coordinates fall in the reddish orange region of chromaticity diagram. From these results, it is suggested that the studied powders may be used for white light generation with the excitation of blue light (450 nm).

The fig.7 shows the frequency dependence of the real part ϵ' of the dielectric constant and loss factor ($\tan\delta$) values as a function of $\log(\omega)$ for the host SrTiO₃ pellet and was studied in the frequency range 100Hz – 1MHz at room temperature. The dielectric constant was calculated using this formula $\epsilon' = Cd/\epsilon_0 A$ where C is the capacitance of the sample, d is the thickness, ϵ_0 is the vacuum dielectric constant (8.85×10^{-12} farad/m) and A is the cross-sectional area of the sample. The dielectric constant of SrTiO₃ is found to be 1880 (by using a formula) Dielectric loss can be calculated using this formula $\tan\delta = \epsilon''/\epsilon'$ where ϵ'' is the imaginary part of the dielectric constant and ϵ' is the real part of the dielectric constant. The value of dielectric loss is found to be 156×10^{-4} . From the figures it is observed that dielectric constant (ϵ') and dielectric loss ($\tan\delta$) values are decreasing with an increase in frequency of strontium titanate ceramic powder. When the frequency of the applied electric field increased to a certain value that is more than the frequency of dielectric relaxation polarization, the contribution of dielectric relaxation polarization to dielectric constant decreased, which is attributed to a Maxwell-Wagner relaxation behavior [10-15]. Hence the dielectric constant decreased as the frequency increased, and dielectric loss was evident in the dielectric constant. Also, the dielectric constant and loss increased with increasing due to less contribution of ions in the direction of applied electric field. The inset figure shows that the AC conductivity of the SrTiO₃ ceramic powder, pellet as a function of $\log(\omega)$ at room temperature. The AC conductivity was calculated using this formula $\sigma_{ac} = \epsilon_r \epsilon_0 \omega \tan\delta$ where ϵ_r is the vacuum dielectric constant (8.85×10^{-12} farad/m), ϵ_r is the relative dielectric constant, ω is the angular frequency ($\omega = 2\pi\nu$) and $\tan\delta$ is the loss factor. The AC conductivity of the SrTiO₃ is found to be 6.1×10^2 S/cm. From the figure it is observed that the AC conductivity is increasing with increasing the frequency. At high frequency, the conductivity is increased. Where it obeys the power law relation that is $\sigma(\omega) = A\omega^s$; ω is the angular frequency of AC signal.

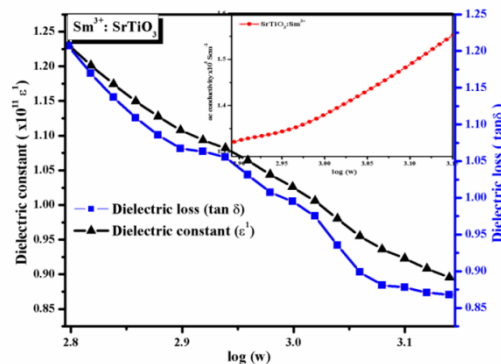


Fig.8 Dielectric constant (ϵ'), loss factor ($\tan\delta$) & ac conductivity (inset figure) of Sm³⁺: SrTiO₃ ceramic powder

The fig.8 shows that the dielectric constant ϵ' and loss factor $\tan\delta$ values as a function of $\log(\omega)$ for the Sm³⁺: SrTiO₃ pellet and was studied in the frequency range 100Hz – 1MHz at room temperature. From the figures it is observed that dielectric constant (ϵ') and dielectric loss ($\tan\delta$) values are decreasing with an increase in frequency of samarium doped strontium titanate ceramic powder. The high dielectric constant is also related to the substitution of Sm³⁺ to Sr²⁺. It is reported that the rare earth doped SrTiO₃ ceramics with dielectric constant is increased compared to that of pure SrTiO₃ value is 1.24×10^{11} , dielectric loss lower than 0.87 and the AC conductivity is 1.32×10^5 S/cm were obtained. Sr vacancies and Ti vacancies charge compensation mechanism is reasonable for high dielectric constant trivalent rare-earth doped SrTiO₃ ceramics. In this work, that trivalent ions Sm³⁺ replaced the divalent ions Sr²⁺ at the A-sites of the perovskite lattice would result in Sr-site vacancies to maintain the charge equilibrium. It is believed that a small quantity of Sr-site vacancies will helpful to improve the dielectric constant. It is clear that all doped ceramic powders show higher values than the un doped ceramic powder due to the introduction of localized states [16].

V. CONCLUSION

SrTiO₃ and Sm³⁺: SrTiO₃ ceramic powders were successfully synthesized by the solid-state reaction method. Strontium titanate powder x-ray diffraction analysis confirms the phase transition occurred. The strontium titanate can be changed into cubic to tetragonal nature. The crystalline size of the powder has been calculated by using the Scherer's equation. The atomic arrangement of SrTiO₃ was visualized by the Visualization for Electronic and Structural Analysis (VESTA). The SEM & EDS image shows the morphological and elemental analysis. By using the SEM we can

calculate the grain size for both SrTiO₃ and Sm³⁺: SrTiO₃ powders. The samarium doped strontium titanate grain size has been increased compared to pure strontium titanate, due to because of by adding the rare earth ion. From the Raman analysis, we have evaluated the prounon properties and structural phase transition. A prominent red-orange emission peak observed at 602 nm (⁴G_{5/2} → ⁶H_{7/2}) from the photoluminescence spectrum of samarium doped strontium titanate. The CIE chromacity diagram shows the orange, red region by using the x and y co-ordinates (0.47 & 0.36). The dielectric properties of SrTiO₃ and Sm³⁺: SrTiO₃ ions also studied. The obtained results of Sm³⁺: SrTiO₃ ceramics indicate its potential as a promising reddish orange optical material for its use in certain electronic devices. Sm³⁺ doped SrTiO₃ can be considered as a promising dielectric material due to the increased dielectric constant, dielectric loss and increasing Ac conductivity values compared to the un doped SrTiO₃. Therefore Sm³⁺: SrTiO₃ is good dielectric material and it can be used in energy storage applications.

REFERENCES

- [1] M. A. Saifi and L. E. Cross, "Dielectric properties of strontium titanate at low temperatures," Phys. Rev. B, vol. 2, pp. 677- 684, Aug. 1970.
- [2] T. Sakudo and H. Unoki, "Dielectric Properties of SrTiO₃ at Low Temperatures," Phys. Rev. Lett., Vol.26, pp. 851-854, April. 1971.
- [3] Chourasia Rashmi and O.P. Shrivastava, "Crystal structure modeling, electrical and microstructural characterization of manganese doped barium zirconium titanate ceramics", Polyhedron, vol. 30, pp. 738-745 Jan. 2011.
- [4] D.D. Ligny and P. Richet, "High-temperature heat capacity and thermal expansion of SrTiO₃ and SrZrO₃ perovskites", Phys. Rev. B, vol.53, pp. 1-6, Jan. 2013.
- [5] T.K.Song,J.Kim,S.I.Kwun, "SRTIO₃ NANOCRYSTALS", Solid State Communications, Vol. 97(2), pp. 143-147, Oct. 1996.
- [6] Khalid Mujasam Bato, Shalendra Kumar, and Chan Gyan Lee, "Alimuddin, Study of ac impedance spectroscopy of Al doped MnFe₂-2xAl₂xO₄", J. Alloy. Compd. Vol. 480, pp. 596-602, Oct.2009.
- [7] M.Schumacher,G.W.Dietz, R. Waser, "Electrode influence on the charge transport through SrTiO₃ thin films", Integrated Ferroelectrics, vol. 10, pp. 231-245 Oct. 1995.
- [8] S.Mochizuki,F.Fujishiro,andS.Minami,"Photoluminescence and reversible photo- induced spectral change of SrTiO₃", J. Phys. C vol. 17, pp. 923-948, Jun. 2005.
- [9] E.A.V. Ferri, J.C. Sczancoski, L.S. Cavalcante, E.C. Paris, J.W.M. Espinosa, A.T. de Figueiredo, P.S. Pizani, V.R.Mastelaro, J.A.Varela and E.Longo, "Photoluminescence behavior in MgTiO₃ powders with vacancy/distorted clusters and octahedral tilting", Mater. Chem. & phys.vol.117, pp. 192-198, May. 2009.
- [10] E. Melagiriappa, H.S. Jayanna, and B.K. Chougule, "Dielectric behavior and ac electrical conductivity study of Sm³⁺ substituted Mg -Zn ferrites", J. Mater. Chem. Phys. Vol. 112, pp. 68-73, Jan. 2008.
- [11] T. Badapanda, S. Sarangi, S. Parida, B. Behera, B. Ojha, and S. Anwar, " Frequency and temperature dependence dielectric study of strontium modified Barium Zirconium Titanate ceramics", J. Mater. Sci.: Mater. Electron. Vol.26, pp. 3069-3082, Dec. 2015.
- [12] N. Singh, A. Agarwal, S. Sanghi, and S. Khasa, "Dielectric loss, conductivity relaxation process and magnetic properties of Mg substituted Ni-Cu ferrites", J. Magn. Magn. vol.324, pp. 2506-2511, Oct. 2012.
- [13] A. Dutta, T.P. Sinha, P. Jena, and S. Adak, "Ac conductivity and dielectric relaxation in ionically conducting soda-lime-silicate glasses", J. Non-Cryst. Solids, vol.354, pp. 3952-3957, Nov. 2008.
- [14] R.A. Mondal, B.S. Murthy, and V.R.K. Murthy, "Maxwell-Wagner polarization in grain boundary segregated NiCuZn ferrite", Curr. Appl. Phys.Vol.14, pp. 1727-1733, Aug. 2014.
- [15] A.F. Khan, M. mehmood, A. M. Rana and T. Muhammad, "Effect of Annealing on Structural, Optical and Electrical Properties of Nanostructured Ge Thin Films", Applied Surface Science, vol. 256 (7), pp.2031 - 2037, Nov. 2010.
- [16] Z.Y. Shen, Q.G. Hu, Y.M. Li, Z.M. Wang, W.Q. Luo, Y. Hong, Z.X. Xie, and R.H. Liao, "Structure and dielectric properties of Re_{0.02}Sr_{0.97}TiO₃ (Re = La, Sm Gd, Er) ceramics for high-voltage capacitor applications", J. Am. Ceram. Soc. Vol.96, pp. 2551- 2555, Oct. 2013.